Article pubs.acs.org/JACS

Computational Exploration of a Redox-Neutral Organocatalytic Mitsunobu Reaction

Yike Zou, Jonathan J. Wong, and K. N. Houk*



Cite This: J. Am. Chem. Soc. 2020, 142, 16403-16408



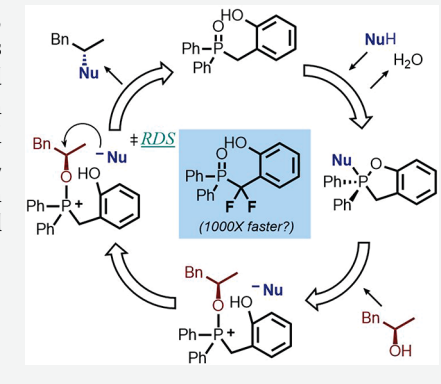
ACCESS

III Metrics & More



Supporting Information

ABSTRACT: The mechanism of the redox-neutral organocatalytic Mitsunobu reaction, catalyzed by (2-hydroxybenzyl)diphenylphosphine oxide, reported by Denton et al., has been studied computationally with ω B97X-D density functional theory. We discovered that the nucleophilic substitution reaction between carboxylate and alkoxyphosphonium ions, to reform the phosphine oxide catalyst, is the rate-determining step of the overall process and is significantly accelerated compared with a general-acid-catalyzed S_N2 reaction. The (2-hydroxybenzyl)diphenylphosphine oxide is regenerated and activated in every catalytic cycle via intramolecular dehydration/cyclization. We also designed several phosphine oxide catalysts that we predict to be more effective catalysts.



■ INTRODUCTION

The Mitsunobu reaction converts an alcohol into a variety of derivatives with inversion of configuration at the carbinol carbon. Alcohols are converted into esters, ethers, amines, amides, and related derivatives. Due to this advantage, Mitsunobu reactions have been widely applied not only in the field of small molecule synthesis^{2,3} but also in the field of bioorganic chemistry, such as structural modifications of saccharides, ⁴ peptides, ⁵ and nucleic acids, ⁶ and also in polymer synthesis.7 However, a major drawback of conventional Mitsunobu reactions is that stoichiometric amounts of the azodicarboxylate and phosphine reagents must be used, and the hydrazine and phosphine oxide side products are not easily separated from the crude product mixtures (Figure 1A), although various methods have been developed to address this issue.8 In last few decades, the Mitsunobu reaction has been made catalytic, first based on the redox cycling of the azodicarboxylate reagent and then catalytic in the phosphine 10 (Figure 1B). In spite of the advantages of these catalytic protocols, a stoichiometric amount of oxidant or reductant must still be used.

In 2019, Denton et al. reported a fully catalytic and redoxneutral Mitsunobu reaction protocol using only a catalytic amount of an organophosphine oxide catalyst (Figure 1C).11 The phosphine oxide, usually the byproduct of the Mitsunobu reactions, is now the catalyst. This protocol generates water as the only side product while still retaining merits of the classical Mitsunobu reaction, such as outstanding stereochemical control and excellent substrate tolerance.

Mitsunobu and co-workers studied various intermediates experimentally and proposed a reaction pathway^{1,3} for the A. Classical Mitsunobu reactions

$$\underbrace{\mathsf{NUPh}_{\mathsf{R}_1}^{\mathsf{OH}} + \mathsf{NUH}}_{\mathsf{R}_2} \underbrace{\overset{\mathsf{DEAD}\,\,(1\,\,\mathrm{eq.})}{\mathsf{PPh}_3\,\,(1\,\,\mathrm{eq.})}}_{\mathsf{PPh}_3\,\,(1\,\,\mathrm{eq.})} \underbrace{\overset{\mathsf{Nu}}{\mathsf{R}_1}}_{\mathsf{R}_2} + \underbrace{\mathsf{EtO}_2\mathsf{C}}_{\mathsf{H}} \overset{\mathsf{N}}{\mathsf{N}_1} \underbrace{\mathsf{EtO}_2\mathsf{C}}_{\mathsf{H}} + \underbrace{\mathsf{OPPh}_3}_{\mathsf{H}}$$

B. Redox-cycling catalytic Mitsunobu reactions

$$\begin{array}{c} \text{OH} \\ \text{R_1} \\ \end{array} \begin{array}{c} \text{OH} \\ \text{R_2} \\ \end{array} \begin{array}{c} \text{NuH} \\ \text{oxidant,} \\ \text{PR_3} \\ \text{oxidant,} \\ \text{PR_3} \\ \end{array} \begin{array}{c} \text{Nu} \\ \text{OH} \\ \text{R_1} \\ \text{R_2} \\ \end{array} \begin{array}{c} \text{OH} \\ \text{R_2} \\ \text{R_2} \\ \end{array} \begin{array}{c} \text{PR_3} \\ \text{(cat.)} \\ \text{reductant,} \\ \text{R_1} \\ \text{R_2} \\ \end{array} \begin{array}{c} \text{Nu} \\ \text{reductant,} \\ \text{R_2} \\ \end{array}$$

C. Redox-free catalytic Mitsunobu reactions

Figure 1. Mitsunobu reactions.

original Mitsunobu reaction which involves four stages (Figure 2A): (i) generation of quaternary phosphonium-azoate zwitterionic intermediate 2 from the phosphine and azodicarboxylate reactants; (ii) protonation of 2 leading to hydrazyl phosphonium 3 and nucleophilic Nu-; (iii) alcohol attack on the phosphorus center of 3 leading to alkoxy-

Received: July 12, 2020 Published: September 2, 2020



A. Mechanism of a classical Mitsunobu reaction

B. Mechanism of a redox-free catalytic Mitsunobu reaction

Figure 2. Mechanism of a classical and a redox-neutral catalytic Mitsunobu reaction.

phosphonium salt 4; (iv) an essentially intramolecular S_N2 displacement by the nucleophile anion in an ion pair to generate product 5. The acidity of the nucleophile (NuH), often a carboxylic acid, significantly influences the reaction pathway and outcome. 12 This mechanism was further elaborated¹³ by multiple research groups via investigations of unusual reaction outcomes, ¹⁴ factors that affect reaction rate, ^{10c,15} reactive intermediates, ¹⁶ and stereochemical outcomes.¹⁷ Nevertheless, the structures of various hypervalent phosphorus intermediates involved in the Mitsunobu reaction are largely unknown. QM calculations allow systematic investigations of reaction pathways and reveal the structural features of various intermediates. To date, the only reported computational studies of the Mitsunobu reaction were by Anders et al. in 2005 using PH3 as a model reagent and methanol as the alcohol. 18 Comprehensive DFT studies were carried out to describe the interconversions of different phosphonium intermediates and ligand exchange processes on the phosphorus center, which established a detailed reaction pathway. Interestingly, both retention and inversion pathways are predicted to occur with different phosphines and substrates, but the inversion path is favored with the usual substrates and conditions. 18

■ COMPUTATIONAL METHODS

Density functional theory (DFT) calculations were performed with Gaussian 09. ¹⁹ The geometry of each species was optimized using the ωB97X-D functional ²⁰ and the 6-311G(d,p) basis set with the CPCM solvation model for toluene. For the reaction pathway involving triflic anhydride (Figure S1), the calculations were performed with the CPCM solvation model for chloroform. Frequency calculations were performed at the same theorical level as for geometry optimizations to verify the stationary points as either minima or first-order saddle points on the potential energy surface as well as to obtain thermal Gibbs free energy corrections at 298 K. All DFT calculations were with an ultrafine integration grid. Optimized structures are presented using CYLview. ²² Conformational searches were performed with the Merck molecular force field (MMFF) implemented in the Spartan 16 program package ²³ to locate the lowenergy conformations.

RESULTS AND DISCUSSION

Denton et al. proposed a mechanism and catalytic cycle (Figure 2B) for the catalytic reaction that involves (i) dehydrative generation of cyclo-phosphonium salt 6 from phosphine oxide catalyst 1, (ii) generation of alkoxy-phosphonium salt 7 via ring opening of 6 and proton transfer

from the alcohol, and finally (iii) a $S_{\rm N}2$ attack from the nucleophile to generate the product with the inverted stereochemistry and regeneration of the phosphine oxide catalyst. Experiments were performed to support this mechanism that include structure—activity relationship studies of the catalyst, isotope labeling, and capture of the reactive species. The first cyclo—dehydration step was proposed to be the turnover-limiting step.

Extensive experimental studies showed that phosphonium 6 is the active species prior to the S_N2 reaction. A key phosphonium species 6 was captured with trifluoromethanesulfonate counterion and characterized by NMR experiments. Dehydrative generation of 6 was suggested to be the ratelimiting step. Intermediate 6 was assumed to be water sensitive, and Dean-Stark azeotropic distillation was required during the reaction. However, it is not clear that the dehydration step is rate determining since no kinetic studies are available. In contrast to the mild conditions of conventional Mitsunobu reactions, this catalytic Mitsunobu reaction is water sensitive and requires high temperature (reflux in toluene or xylenes) and extended reaction time (16-120 h) to achieve a synthetically satisfying yield. With these considerations in mind, we launched a computational study on this redox-neutral catalytic Mitsunobu reaction, in particular focusing on the initial dehydration step and the final substitution step, applying DFT calculations using the ω B97X-D functional with the 6-311G(d,p) basis set.²⁴

We explored the reaction of (R)-1-phenylpropan-2-ol, involving the experimental results where a (>99% ee) sample reacts with 2,4-dinitrobenzoic acid to produce (S)-ester 10 in 92% yield and 96% ee (Figure 3). 10 Initially, phosphine oxide 1 forms a hydrogen-bonded complex (11) with acid 9. This process is exergonic by 1.8 kcal/mol. Complex 11 is assigned as a minimum on the energy landscape. Addition of the phenolic OH to the P=O double bond can proceed via transition state 12, in which the P-O single bond forming distance is 2.4 Å, with an energy barrier of 23.3 kcal/mol. There may be a variety of mechanisms for this to occur by adventitious acid or base catalysis, and we consider this an upper limit to the barrier for formation of 13 from 9. Notably in this process, the tetrahedral geometry of 1 changes to the trigonal bipyramidal 13. Transition state 12 also possesses a trigonal bipyramidal geometry with the hydroxy group occupying an equatorial position. Due to the apicophilicity of a hydroxy group on an oxo--phosphorane, 25 13 isomerizes into 14 with the -OH in the axial position with a 5.7 kcal/mol decrease in free energy. This isomerization process can be achieved via either a Berry pseudorotation or a turnstile rotation mechanism with only a few kcal/mol barrier²⁶ or by conformational change via rotation of the C3-C4 bond with a ca. 4 kcal/mol barrier acquired from dihedral scanning (Figure S4, Supporting Information). Note that the bond length of a P-O single bond is typically 1.43-1.67 Å.²⁷ However, the Xray structures of similar cyclic phosphorane species have been reported with some P-O bond distances being more than 1.8 Å. 28 In cyclic oxo-phosphoranes 13 and 14, the P-O lengths are more than 1.8 Å.

We studied **15** and **16** and found that the natural bond orbital (NBO) bond orders between P and O1 are 0.41 and 0.47 for **15** and **16**, respectively. Hirshfeld charge analyses (Figure S2, Supporting Information) show a large charge separation between P and O1 (ca. +0.3 and -0.3 respectively); there is a partial covalent and ionic character between P-O1 of

Later 2, 1741, 141, 200, 140, 100, 175, 200, 000, 240, 2

16101

Figure 3. DFT investigation of the initial step with ω B97X-D/6-311G(d,p)/CPCM(toluene).

15 and 16. The bonding parameters of various related phosphorane species (vide infra) were also investigated. In general, when the two axial ligands are both oxygen groups, the more basic group forms a P–O single bond whereas the less basic group forms a partial (approximately one-half) P–O bond. These results are summarized in Figure S3 of the Supporting Information.

Having established the nature of the phosphorane intermediate, we studied the dehydration step which leads to the active phosphorane species. Dehydration of the phosphorane –OH group is mediated by the carboxylic acid. Denton et al. speculated that this dehydration was likely to be the rate-determining step. Dehydration of the cis intermediate (13, Figure 4) proceeds via transition state 17 with a free energy barrier of 31.6 kcal/mol and leads to 19 as a high-energy intermediate (28.6 kcal/mol). These are indeed very high barriers. However, dehydration from the trans intermediate (14) takes place with a free energy barrier of only 22.0 kcal/mol via transition state 18 which leads to 20, which has a free energy of 14.4 kcal/mol. The preference for the dehydration of 14 is due to the trans effect of the phosphoranes on which water is more prone to dissociate when being trans to the

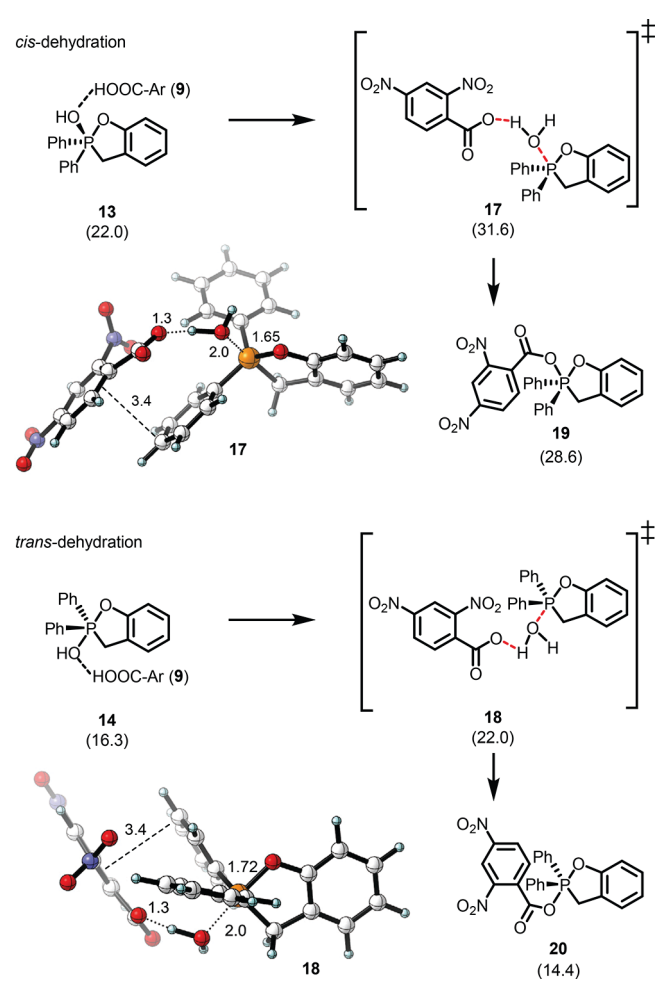


Figure 4. Dehydration and coordination of carboxylate to phosphorus.

phenoxy oxygen.²⁹ The dehydration step generates a trigonal bipyramid **20** with the carboxylate and phenoxide apical.³⁰ The relative energy of **20** is 14.4 kcal/mol, which explains why it was not observed in NMR experiments.¹⁰ In contrast, the change of the apical anion from carboxylate to triflate resulted in **S1** (see Supporting Information) with a -23.3 kcal/mol relative free energy, explaining why this species could be observed and characterized experimentally.

From 20, the reaction of alcohol 8 to form 23 occurs. This process can be initiated by formation of the hydrogen-bonded complex 21 (Pathway A, Figure 5). Phosphorane ring opening of 21 followed by association of the alkoxide upon proton transfer leads to 22. Reassociation of the phenoxy oxygen and dissociation of the carboxylate with proton transfer then leads to 23. Alternatively, as depicted in Pathway B, hydrogen bonding of 8 with 20 leads to complex 24 (Figure 5, Pathway B) with a 2.4 kcal/mol decrease in free energy. Proton transfer from alcohol to carboxylate of 24 takes place almost barrierlessly via transition state 25 (13.5 kcal/mol). We computed the energetics for various steps but generally did not attempt to compute proton transfers that might involve solvent assistance and tunneling. ³¹ Phosphorane 23 (11.8 kcal/mol) can equilibrate with 24 (12.0 kcal/mol).

Complex 26 (Figure 6) is generated from 23 via proton transfer from carboxylic acid to the phenoxide and ring opening of the phosphorane.³² This complex, 26, has the

Later 2, 1741, 141, 200, 140, 100, 175, 200, 000, 240, 2

Pathway A: ligand exchange by ring-opening

Pathway B: ligand exchange by protonation/dissociation

$$O_2N$$
 Ph
 Ph
 O_2N
 Ph
 Ph
 O_2N
 Ph
 Ph
 O_2N
 O_2N

Figure 5. Ligand exchange on the phosphorus center.

carboxylate set up for the $S_{\rm N}2$ transition state 27 that is relatively high in energy (32.6 kcal/mol). While this rate-determining step is rather slow, 27 is low compared with the uncatalyzed (or general-acid-catalyzed) reaction barrier (from 28 to 29, which we compute to be 43.3 kcal/mol). The reasonably harsh reaction conditions [xylenes (bp ca. 140 °C), reflux, 72 h] are necessary to overcome the 32.6 kcal/mol $S_{\rm N}2$ barrier. Product 10 is generated with inverted stereochemistry and regeneration of phosphine oxide 1.

Redesign of Phosphine Oxide Catalyst. Computational design is an essential component of rational design of catalysts and has achieved considerable success.³³ We attempted to redesign the phosphine oxide catalyst to decrease the activation energy of the rate-determining 2 step and increase the activity of the catalyst. Electron-withdrawing groups on the aromatic substituents of the phosphorus should make the

$$O_2N$$
 O_2N
 O_2N

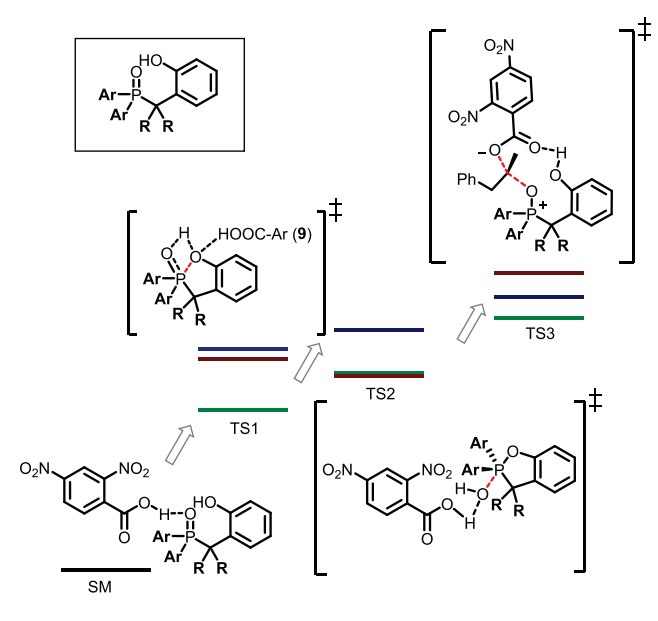
Figure 6. Nucleophilic substitution steps.

corresponding phosphine oxide a better leaving group and thereby afford a faster S_N2 reaction. We first replaced the bisphenyl substituents with bis-perfluorophenyl (32); this substitution causes an increase in the energy of the cyclization (33) and dehydration (34) transition states but a 2.8 kcal/mol decrease in the rate-determining S_N2 activation barrier (35) (Figure 7). We also replaced the benzylic methylene hydrogens with fluorine atoms (36). This resulted in a significant decrease in both the cyclization (37) and the S_N2 activation barrier (39). All three transition states (37, 38, and 39) are stabilized the most in low-polar solvent such as toluene.³⁴ Both the perfluorophenyl catalyst of 32 and the difluoromethylene catalyst of 36 are predicted to be more active than the original catalyst with 36 being the best. Catalyst 36 likely can be synthesized from commercially available phosphine oxide 30 and known compound 31.35

CONCLUSIONS

To summarize, the mechanism of a redox-neutral organocatalytic Mitsunobu reaction has been investigated. The steps proposed by Denton et al. are verified, and the bonding details in the phosphorane intermediates were determined. This protocol provides a novel way to generate the active phosphonium species from dehydration of the phosphine oxide. The dehydration process, originally speculated to be rate

Later 2, 1741, 141, 200, 140, 100, 175, 200, 000, 240, 2



species	SM	TS1	TS2	TS3
Ar=Ph, R =H	11 , (0.0)	12 , (23.3)	18 , (22.0)	27 , (32.6)
$\mathbf{Ar}=\mathbf{C}_{6}\mathbf{F}_{5},$ $\mathbf{R}=\mathbf{H}$	32 , (0.0)	33 , (24.4)	34 , (26.1)	35 , (29.8)
Ar =Ph, R =F	36 , (0.0)	37 , (17.3)	38 , (22.0)	39 , (27.8)

Figure 7. Redesign of the catalyst for a higher activity.

determining, occurs with a relatively low energy barrier. The final $S_{\rm N}2$ step from an ion-pair intermediate is the rate-determining step. We studied other derivatives of the catalyst and predict improved catalysts with faster rates involving fluorine substituents.

ASSOCIATED CONTENT

Supporting Information

The Supporting Information is available free of charge at https://pubs.acs.org/doi/10.1021/jacs.0c07487.

Energies and coordinates of computed structures (PDF)

AUTHOR INFORMATION

Corresponding Author

K. N. Houk – Department of Chemistry and Biochemistry, University of California, Los Angeles, California 90095-1569, United States; orcid.org/0000-0002-8387-5261; Email: houk@chem.ucla.edu

Authors

Yike Zou – Department of Chemistry and Biochemistry, University of California, Los Angeles, California 90095-1569, United States; occid.org/0000-0003-4380-7827

Jonathan J. Wong — Department of Chemistry and Biochemistry, University of California, Los Angeles, California 90095-1569, United States

Complete contact information is available at: https://pubs.acs.org/10.1021/jacs.0c07487

Notes

The authors declare no competing financial interest.

ACKNOWLEDGMENTS

We are grateful to the National Science Foundation (Grant CHE-1764328) for financial support of this research. We thank Prof. Brian Stoltz, Prof. Ohyun Kwon, and insightful reviewers for helpful discussions. All calculations were performed on the Hoffman2 cluster at the University of California, Los Angeles, and the Extreme Science and Engineering Discovery Environment (XSEDE), which is supported by the National Science Foundation (Grant OCI-1053575).

REFERENCES

- (1) (a) Mitsunobu, O.; Yamada, M.; Mukaiyama, T. Preparation of esters of phosphoric acid by the reaction of trivalent phosphorus compounds with diethyl azodicarboxylate in the presence of alcohols. Bull. Chem. Soc. Jpn. 1967, 40 (4), 935–939. (b) Mitsunobu, O.; Yamada, M. Preparation of esters of carboxylic and phosphoric acid via quaternary phosphonium salts. Bull. Chem. Soc. Jpn. 1967, 40 (10), 2380–2382. (c) Mitsunobu, O.; Eguchi, M. Preparation of carboxylic esters and phosphoric esters by the activation of alcohols. Bull. Chem. Soc. Jpn. 1971, 44 (12), 3427–3430. (d) Mitsunobu, O.; Wada, M.; Sano, T. Stereospecific and stereoselective reactions. I. Preparation of amines from alcohols. J. Am. Chem. Soc. 1972, 94 (2), 679–680.
- (2) Swamy, K. C. K.; Kumar, N. N. B.; Balaraman, E.; Kumar, K. Mitsunobu and related reactions: advances and applications. *Chem. Rev.* **2009**, *109* (6), 2551–2651.
- (3) Mitsunobu, O. The use of diethyl azodicarboxylate and triphenylphosphine in synthesis and transformation of natural products. *Synthesis* **1981**, *1981* (01), 1–28.
- (4) Roush, W. R.; Lin, X. F. Studies on the synthesis of antibiotics highly stereoselective synthesis of aryl 2-deoxy-beta-glycosides via the Mitsunobu reaction and synthesis of the olivomycin A-B disaccharide. *J. Am. Chem. Soc.* **1995**, *117* (8), 2236–2250.
- (5) Wisniewski, K.; Koldziejczyk, A. S.; Falkiewicz, B. Applications of the Mitsunobu reaction in peptide chemistry. *J. Pept. Sci.* **1998**, *4* (1), 1–14.
- (6) (a) Malecki, E.; Knies, C.; Werz, E.; Rosemeyer, H. Mitsunobu reactions of 5-fluorouridine with the terpenols phytol and nerol: dna building blocks for a biomimetic lipophilization of nucleic acids. *Chem. Biodiversity* **2013**, *10* (12), 2209–2220. (b) Falkiewicz, B. Application of mitsunobu reaction to solid-phase peptide nucleic acid (PNA) monomer synthesis. *Nucleosides, Nucleotides Nucleic Acids* **2002**, *21* (11–12), 883–889.
- (7) (a) Zong, K. W.; Madrigal, L.; Groenendaal, L.; Reynolds, J. R. 3,4-Alkylenedioxy ring formation via double Mitsunobu reactions: an efficient route for the synthesis of 3,4-ethylenedioxythiophene (EDOT) and 3,4-propylenedioxythiophene (ProDOT) derivatives as monomers for electron-rich conducting polymers. *Chem. Commun.* **2002**, 21, 2498–2499. (b) Kim, J.; Yoon, D.; Lee, S. H.; Ko, S.; Lee, Y. S.; Zong, K. An efficient synthesis of thiophene/pyrrole-fused crown ethers using mitsunobu reaction for potential application to sensory electroactive polymers. *Bull. Korean Chem. Soc.* **2006**, 27 (11), 1910–1912.
- (8) (a) Dembinski, R. Recent advances in the Mitsunobu reaction: Modified reagents and the quest for chromatography-free separation. Eur. Eur. J. Org. Chem. 2004, 2004 (13), 2763–2772. (b) Proctor, A. J.; Beautement, K.; Clough, J. M.; Knight, D. W.; Li, Y. F. Chromatography-free product separation in the Mitsunobu reaction. Tetrahedron Lett. 2006, 47 (29), 5151–5154. (c) Qi, N.; Guo, J.; He, Y. Progress in separation-friendly mitsunobu reactions. Chin. J. Org. Chem. 2016, 36 (12), 2880–2887. (d) Dandapani, S.; Curran, D. P. Separation-friendly Mitsunobu reactions: a microcosm of recent developments in separation strategies. Chem. Eur. J. 2004, 10 (13), 3130–3138. (e) Harned, A. M.; He, H. S.; Toy, P. H.; Flynn, D. L.; Hanson, P. R. Multipolymer solution-phase reactions: Application to

Later 2, 774. 121 2 - 140 1001 72 22 0-07407

- the Mitsunobu reaction. *J. Am. Chem. Soc.* **2005**, 127 (1), 52–53. (f) Arnold, L. D.; Assil, H. I.; Vederas, J. C. Polymer-supported alkyl azodicarboxylates for mitsunobu reactions. *J. Am. Chem. Soc.* **1989**, 111 (11), 3973–3976.
- (9) But, T. Y. S.; Toy, P. H. Organocatalytic Mitsunobu reactions. J. Am. Chem. Soc. 2006, 128 (30), 9636–9637.
- (10) (a) Buonomo, J. A.; Aldrich, C. C. Mitsunobu reactions catalytic in phosphine and a fully catalytic system. *Angew. Chem., Int. Ed.* **2015**, *54* (44), 13041–13044. (b) Hirose, D.; Gazvoda, M.; Kosmrlj, J.; Taniguchi, T. The "fully catalytic system" in Mitsunobu reaction has not been realized yet. *Org. Lett.* **2016**, *18* (16), 4036–4039. (c) Hirose, D.; Gazvoda, M.; Kosmrlj, J.; Taniguchi, T. Advances and mechanistic insight on the catalytic Mitsunobu reaction using recyclable azo reagents. *Chem. Sci.* **2016**, *7* (8), 5148–5159.
- (11) Beddoe, R. H.; Andrews, K. G.; Magne, V.; Cuthbertson, J. D.; Saska, J.; Shannon-Little, A. L.; Shanahan, S. E.; Sneddon, H. F.; Denton, R. M. Redox-neutral organocatalytic Mitsunobu reactions. *Science* **2019**, 365 (6456), 910–914.
- (12) Dodge, J. A.; Trujillo, J. I.; Presnell, M. Effect of the acidic component on the Mitsunobu inversion of a sterically hindered alcohol. *J. Org. Chem.* **1994**, *59* (1), 234–236.
- (13) But, T. Y. S.; Toy, P. H. The Mitsunobu reaction: Origin, mechanism, improvements, and applications. *Chem. Asian J.* **2007**, *2* (11), 1340–1355.
- (14) (a) Adam, W.; Narita, N.; Nishizawa, Y. On the mechanism of the "triphenylphosphine-azodicarboxylate (Mitsunobu reaction) esterification. J. Am. Chem. Soc. 1984, 106 (6), 1843–1845. (b) Elson, K. E.; Jenkins, I. D.; Loughlin, W. A. The Hendrickson reagent and the Mitsunobu reaction: a mechanistic study. Org. Biomol. Chem. 2003, 1 (16), 2958–2965.
- (15) (a) Varasi, M.; Walker, K. A. M.; Maddox, M. L. A Revised mechanism for the Mitsunobu reaction. *J. Org. Chem.* **1987**, *52* (19), 4235–4238. (b) Hughes, D. L.; Reamer, R. A.; Bergan, J. J.; Grabowski, E. J. J. A mechanistic study of the Mitsunobu esterification reaction. *J. Am. Chem. Soc.* **1988**, *110* (19), 6487–6491.
- (16) (a) Camp, D.; Jenkins, I. D. Mechanism of the Mitsunobu esterification reaction 0.2. the involvement of (acyloxy)-alkoxyphosphoranes. *J. Org. Chem.* **1989**, 54 (13), 3049–3054. (b) Camp, D.; von Itzstein, M.; Jenkins, I. D. The mechanism of the first step of the Mitsunobu reaction. *Tetrahedron* **2015**, 71 (30), 4946–4948.
- (17) (a) Ahn, C. J.; Correia, R.; DeShong, P. Mechanistic study of the Mitsunobu reaction. *J. Org. Chem.* **2002**, *67* (6), 1751–1753. (b) Ahn, C.; Correia, R.; DeShong, P. Mechanistic study of the Mitsunobu reaction (vol 67, pg 1751, 2002). *J. Org. Chem.* **2003**, *68* (3), 1176–1176.
- (18) Schenk, S.; Weston, J.; Anders, E. Density functional investigation of the Mitsunobu reaction. J. Am. Chem. Soc. 2005, 127 (36), 12566-12576.
- (19) Frisch, M. J.; Trucks, G. W.; Schlegel, H. B.; Scuseria, G. E.; Robb, M. A.; Cheeseman, J. R.; Scalmani, G.; Barone, V.; Mennucci, B.; Petersson, G. A.; Nakatsuji, H.; Caricato, M.; Li, X.; Hratchian, H. P.; Izmaylov, A. F.; Bloino, J.; Zheng, G.; Sonnenberg, J. L.; Hada, M.; Ehara, M.; Toyota, K.; Fukuda, R.; Hasegawa, J.; Ishida, M.; Nakajima, T.; Honda, Y.; Kitao, O.; Nakai, H.; Vreven, T.; Montgomery, J. A., Jr.; Peralta, J. E.; Ogliaro, F.; Bearpark, M.; Heyd, J. J.; Brothers, E.; Kudin, K. N.; Staroverov, V. N.; Kobayashi, R.; Normand, J.; Raghavachari, K.; Rendell, A.; Burant, J. C.; Iyengar, S. S.; Tomasi, J.; Cossi, M.; Rega, N.; Millam, J. M.; Klene, M.; Knox, J. E.; Cross, J. B.; Bakken, V.; Adamo, C.; Jaramillo, J.; Gomperts, R.; Stratmann, R. E.; Yazyev, O.; Austin, A. J.; Cammi, R.; Pomelli, C.; Ochterski, J. W.; Martin, R. L.; Morokuma, K.; Zakrzewski, V. G.; Voth, G. A.; Salvador, P.; Dannenberg, J. J.; Dapprich, S.; Daniels, A. D.; Farkas; Foresman, J. B.; Ortiz, J. V.; Cioslowski, J.; Fox, D. J. Gaussian 09; Gaussian Inc.: Wallingford, CT, 2009.
- (20) Chai, J.-D.; Head-Gordon, M. Long-range corrected hybrid density functionals with damped atom—atom dispersion corrections. *Phys. Chem. Chem. Phys.* **2008**, *10* (44), 6615–6620.

- (21) (a) Barone, V.; Cossi, M. Quantum calculation of molecular energies and energy gradients in solution by a conductor solvent model. *J. Phys. Chem. A* **1998**, *102* (11), 1995–2001. (b) Cossi, M.; Rega, N.; Scalmani, G.; Barone, V. Energies, structures, and electronic properties of molecules in solution with the C-PCM solvation model. *J. Comput. Chem.* **2003**, *24* (6), 669–681.
- (22) Legault, C. Y. CYLview, 1.0b; Universite' de Sherbrooke, 2009; http://www.cylview.org.
- (23) Spartan 16, Wavefunction, Inc., 2016.
- (24) Mardirossian, N.; Head-Gordon, M. Thirty years of density functional theory in computational chemistry: an overview and extensive assessment of 200 density functionals. *Mol. Phys.* **2017**, *115* (19), 2315–2372.
- (25) (a) Wladkowski, B. D.; Krauss, M.; Stevens, W. J. Apicophilicities of substituted oxyphosphoranes: [P(OH)4X, PO-(OH)3X]. *J. Phys. Chem.* **1995**, *99* (13), 4490–4500. (b) Matsukawa, S.; Kajiyama, K.; Kojima, S.; Furuta, S.-y.; Yamamoto, Y.; Akiba, K.-y. A method for determining the difference in relative apicophilicity of carbon-containing substituents of 10-P-5 phosphoranes. *Angew. Chem., Int. Ed.* **2002**, *41* (24), 4718–4722.
- (26) (a) Ugi, I.; Marquarding, D.; Klusacek, H.; Gillespie, P.; Ramirez, F. Berry pseudorotation and turnstile rotation. *Acc. Chem. Res.* 1971, 4 (8), 288–296. (b) Chang, N.-y.; Lim, C. An ab initio study of nucleophilic attack of trimethyl phosphate: factors influencing site reactivity. *J. Phys. Chem. A* 1997, 101 (46), 8706–8713. (c) Moc, J.; Morokuma, K. AB Initio molecular orbital study on the periodic trends in structures and energies of hypervalent compounds: five-coordinated XH5 species containing a group 5 central atom (X = P, As, Sb, and Bi). *J. Am. Chem. Soc.* 1995, 117 (47), 11790–11797.
- (27) Bartell, L. S.; Su, L.-S.; Yow, H. Lengths of phosphorus-oxygen and sulfur-oxygen bonds. Extended Hückel molecular orbital examination of Cruickshank's d.pi.-p.pi. picture. *Inorg. Chem.* **1970**, 9 (8), 1903–1912.
- (28) Jiang, X.-D.; Toya, Y.; Matsukawa, S.; Kojima, S.; Jimenez-Halla, J. O. C.; Shang, R.; Nakamoto, M.; Yamamoto, Y. Synthesis and characterization of a pair of O-fac/O-mer 12-P-6 alkyloxaphosphates with a P-O-C-C four-membered ring. *Chem. Sci.* **2019**, *10* (12), 3466–3472.
- (29) (a) Coe, B. J.; Glenwright, S. J. Trans-effects in octahedral transition metal complexes. *Coord. Chem. Rev.* **2000**, 203, 5–80. (b) Quagliano, J. V.; Schubert, L. The trans effect in complex inorganic compounds. *Chem. Rev.* **1952**, 50 (2), 201–260.
- (30) See Supporting Information Figure S3 for three-dimensional structures of various pentavalent phosphorus species
- (31) Peters, K. S. A Theory-experiment conundrum for proton transfer. Acc. Chem. Res. 2009, 42 (1), 89–96.
- (32) See Supporting Information Figure S6 for detailed studies of the process from 23 to 26
- (33) (a) Houk, K. N.; Cheong, P. H.-Y. Computational prediction of small-molecule catalysts. *Nature* **2008**, 455 (7211), 309–313. (b) Poree, C.; Schoenebeck, F. A Holy Grail in Chemistry: Computational Catalyst Design: Feasible or Fiction? *Acc. Chem. Res.* **2017**, 50 (3), 605–608.
- (34) See Supporting Information for relative energies of 37, 38, and 39 in different CPCM solvent.
- (35) Verhoog, S.; Pfeifer, L.; Khotavivattana, T.; Calderwood, S.; Collier, T. L.; Wheelhouse, K.; Tredwell, M.; Gouverneur, V. Silvermediated 18F-labeling of aryl-CF3 and aryl-CHF2 with 18F-fluoride. *Synlett* **2015**, *27* (01), 25–28.

Law - //d. det - - /10 1001 //- -- 0-0740*